

Parameters identification of a photovoltaic module in a thermal system using meta-heuristic optimization methods

Mohcene Bechouat¹ · Abdelaziz Younsi¹ · Moussa Sedraoui¹ · Youcef Soufi² · Laatra Yousfi³ · Ismail Tabet⁴ · Khaled Touafek⁴

Received: 30 January 2017 / Accepted: 16 October 2017 / Published online: 28 October 2017
© The Author(s) 2017. This article is an open access publication

Abstract Experimental studies confirm that the obtained electrical power by a conventional photovoltaic PV system is progressively degraded when the temperature of its cells is increased. The water-cooled photovoltaic thermal PVT system is therefore proposed to avoid the voltage drop at high temperature. The use of single diode PV/PVT models in simulation software becomes indispensable to analyze its performances where several climatic conditions such as environmental temperature and solar radiation variations

should be considered. An optimal set of PV/PVT model parameters are determined through experimental data using two evolutionary computation algorithms; genetic algorithm and particle swarm optimization algorithm. Furthermore, the robustness of the given PV/PVT model should be analyzed. The predicted electrical properties by the proposed PVT model are compared with those given by the conventional PV model at its operating cell conditions and also at several rigid atmospheric conditions.

✉ Mohcene Bechouat
mohcene.oui@gmail.com

Abdelaziz Younsi
az_younsi@yahoo.fr

Moussa Sedraoui
msedraoui@gmail.com

Youcef Soufi
y_soufi@yahoo.fr

Laatra Yousfi
yousfi_laatra@yahoo.fr

Ismail Tabet
tabet21@yahoo.fr

Khaled Touafek
khaledtouafek@yahoo.fr

Keywords Photovoltaic system · Photovoltaic thermal system · Modelization · Identification · Genetic algorithm · Particle swarm optimization algorithm

Introduction

The main applications of solar energy can be classified into two categories: thermal and photovoltaic systems. In the nature, only 20% of solar radiations incident on a PV module can increase the operating cell temperature, in which its performances are deteriorated [1].

Consequently, the obtained energy conversion is reduced with order of 0.4–0.5% when environmental temperatures are progressively increased [1]. To avoid this drawback, the overheating problem of the conventional PV cells is solved using the proposed cooling system which drops its cell temperatures to those neighboring the nominal temperature range.

The proposed solar system uses the water in the closed circuit in which its cells are cooled down in high temperatures. The advantages of this system are better heat absorption and lower production cost [2, 3]. Therefore, our study focuses on the comparison between the obtained

- ¹ Laboratoire des télécommunications, Université 8 Mai 1945 Guelma, Guelma, Algeria
- ² Labget Laboratory, Department of Electrical Engineering, University of Tebessa, Tebessa, Algeria
- ³ Laboratory Inverses Problems: Modeling, Information and Systems (PI: MIS), University of Tebessa, Tebessa, Algeria
- ⁴ Unité de Recherche Appliquée en Énergies Renouvelables, URAER, Centre de Développement des Énergies Renouvelables, CDER, 47133 Ghardaïa, Algeria



electrical powers by both conventional PV and proposed PVT systems in different atmospheric conditions.

In the modeling step of actual PV/PVT systems, a good choice of the efficient model ensuring more accuracy of the actual system behavior is a key success factor for several analysis studies [4], such as diagnosis, synthesis and robustness of PV/PVT control law step against sensor noises, model parameter uncertainties and PV output power forecast [5]. Therefore, various electrical circuits' oriented PV models have been proposed in the literature providing some optimal models where different intrinsic physical phenomena occurred in the electricity generation process. Among them, the equivalent circuit based upon a single diode is the most commonly adopted model for PV cells, accounting for the photon-generated current and the physics of the P–N junction of the PV cell.

In the design phase of single diode PV models, some unknown parameters should be well optimized such as the photo-generated current, the diode quality factor, the series and parallel resistors and others. An optimal set of these parameters is determined through solving an optimization problem which is previously formulated by the designer. Its fitness metric function (to be minimized) presents the mean square error given through discrepancy value between model prediction and actual measurement for each sampling time.

In the recent years, many researchers have been interested in designing efficient single diode PV models using some evolutionary computation algorithms such as GA or PSO algorithm or others [6, 7]. Among them, Askarzadeh et al. identified the PV model parameters using the Bird Mating Optimizer BMO algorithm [8]. Fialho et al. determined these parameters through some analytical approaches where the PV system was linked to the electric grid [9]. Ogliari et al. estimated the model parameters by adopting the particle filter in the conventional PV power output forecast [10]. Soon and Low identified the single diode KC65T PV model given by three unknown electrical components, which were optimized by the PSO algorithm based upon log barrier constraint [11]. These unknown electrical components have been identified by Qin and Kimball from field test data using PSO algorithm in which both total solar irradiance and environmental temperature variations are taken into account [12]. These parameters have been identified from combining the GA by the Interior-Point Method IPM by Dizqah et al. [13]. Unfortunately, all proposed models are imprecisely described; the actual solar system behaviors when atmospheric conditions are changed in a wide range, particularly at high environmental temperature as well as the robustness of the developed models have not been considered.

This paper investigates the analysis of the above mentioned problem in which two following main contributions

are proposed. The first one is to enhance the obtained electrical properties of the conventional PV system, regardless the effect of various atmospheric conditions. The second one is to decrease the obtained sensitivity of model parameters against environmental temperature variations. Therefore, the obtained electrical properties become depending only on the total solar irradiance variations. As a result, the validity of the proposed model will be extended in wide time range for different weathers such as hot and hazy weathers. The latter presents an important capital, especially, in synthesis control laws ensuring a good tracking of maximum power point MPPT.

The current paper starts in “Tools used for optimization” by introducing the mechanism of both GA and PSO algorithm. In “Circuit model of PV/PVT cells”, the design problem of single diode PV/PVT models is formulated. Its model parameters are then determined through experimental data recorded at different operating points in the “Experimental tests and study cases”. Robustness analysis of obtained PV/PVT models is established where other experimental data recorded at high temperatures and different total solar irradiances are taken into account. Finally, the current paper is ended by a conclusion given in “Conclusion”.

Tools used for optimization

GA optimization

The GA is a heuristic method that simulates the biological evolution, browsing the parameter space. The design of set model parameters are changed according to an evolutionary process based upon genetic rules where some chromosomes may be modified (crossover, mutation, selection..., etc.). In the optimization problem, each variable defines a gene in chromosome. However, the set of chromosomes evolves by different operations modeled on genetic laws to an optimal chromosome [6]. The GA algorithm procedure consists of the following steps:

Step 1: Generate randomly N_p chromosomes on initial population in the search space with

$$\text{chromosome}_\ell = [X_1, \dots, X_n] \text{ where } X_{\min} < X_{1,\dots,n} < X_{\max} \text{ and } \ell = 1, 2, \dots, N_p.$$

Step 2: Calculate the fitness function for each chromosome.

Step 3: Apply the following operators:

- Perform reproduction, i.e., select the best chromosomes with probabilities based upon its fitness function values.
- Perform crossover on chromosomes selected in the above step by crossover probability.



- c. Perform mutation on chromosomes generated in the above step by mutation probability.

Step 4: If the stopping condition is reached or the optimum solution is obtained, the process can be stopped. Otherwise, repeat Steps 2–4 until the stop condition is achieved.

Step 5: Get the optimal solution X^* corresponding to the best fitness function value $X^* = \min_{X_i^j} (J(X_i^j), \forall i, j)$.

PSO optimization

PSO is a meta-heuristic optimization method presented, for the first time, by Kennedy and Eberhart [14]. Their idea was inspired through the social behavior and the ability of a bird flocking or a fish migration. The PSO algorithm uses a swarm consisting of $n_p \in \mathbb{N}$ articles, i.e., $(X_i)_{i=1,2,\dots,n_p}$, to search the sub-optimal solution $X^* \in \mathbb{N}^{q \times 1}$ that minimizes the fitness function $J(X) \in \mathbb{R}$. The position and velocity vectors of i th particle are, respectively, given by $X_i = (X_{i,1}, X_{i,2}, \dots, X_{i,q})^T$ and $V_i = (V_{i,1}, V_{i,2}, \dots, V_{i,q})^T$. These vectors are evolved through the following updated laws:

$$\begin{cases} V_i^{\ell+1} = c_0 \cdot V_i^\ell + c_1 \cdot r_{1,i}^\ell \cdot (X_i^{\text{best},\ell} - X_i^\ell) + c_2 \cdot r_{2,i}^\ell \cdot (X_{\text{swarm}}^{\text{best},\ell} - X_i^\ell) \\ X_i^{\ell+1} = X_i^\ell + V_i^{\ell+1} \end{cases} \quad (1)$$

where $\ell = 1, 2, \dots, \ell_{\max}$ and ℓ_{\max} is the maximum number of iterations that should previously chosen by the user [8, 9]. c_0, c_1 and c_2 are, respectively, the inertia factor, the cognitive (individual) and the social (group) learning rates. $r_{1,i}^\ell$ and $r_{2,i}^\ell$ are random numbers that are uniformly distributed in $[0, 1]$. $X_i^{\text{best},\ell}$ and $X_{\text{swarm}}^{\text{best},\ell}$ are, respectively, the best previously obtained position of the particle i and the best obtained position in the entire swarm at the current iteration ℓ where [15, 16]:

$$\begin{cases} X_i^{\text{best},\ell} = \min_{X_i^j} \{J(X_i^j), 0 \leq j \leq \ell\} \\ X_{\text{swarm}}^{\text{best},\ell} = \min_{X_i^j} \{J(X_i^j), \forall i\} \end{cases} \quad (2)$$

The PSO algorithm consists of the following step-procedures [16]:

Step 1: Initialize the n_p particles with randomly chosen position, which should be previously constrained by $\Omega \in (X_{\min}, X_{\max})$ where $X_{\min} \leq X_i \leq X_{\max}$. Afterward, evaluate the corresponding objective function at each position. Finally, set the iteration number $\ell = 0$ and determine the initial solutions $X_i^{\text{best},0}$ and $X_{\text{swarm}}^{\text{best},0}$ using Eq. (2). Go to the next step.

Step 2: Check termination criterion. If it is satisfied, the algorithm terminates with the solution. Otherwise, go to the next step.

Step 3: Apply updates (1) and (2) to all particles and evaluate the corresponding objective function at each position again. Afterward, set the iteration number $\ell \leftarrow \ell + 1$ and determine $X_i^{\text{best},\ell}$ and $X_{\text{swarm}}^{\text{best},\ell}$. Go back to step 2. For simplicity, the termination criterion in step 2 is set as a maximum number of iteration ℓ_{\max} .

Circuit model of PV/PVT cells

Mathematical model of PV/PVT modules

The following equivalent electrical circuit based on a single diode is commonly used in modeling step of PV/PVT cells:

According to Fig. 1, the electrical circuit model of PV/PVT cells consists of a current source assembled in parallel with a diode. A series resistor and a parallel resistor are added to describe the dissipation phenomena inside PV/PVT cells [17–19]. According to the equivalent circuit, the following expressions are established [20–22]:

$$I_{pv} = I_{ph} - I_D - \frac{V_{pv} + R_s \cdot I_{pv}}{R_p}, \quad (3)$$

where I_{ph} the photo-generated current, I_{pv} and V_{pv} are, respectively, the output current and the output voltage provided by the solar cell. I_D the diode current given by:

$$I_D = I_0 \cdot \left(-1 + e^{\left[q \frac{V_{pv} + R_s \cdot I_{pv}}{K \cdot T_a} \right]} \right), \quad (4)$$

where I_0 is the reverse saturation current of the diode defined by:

$$I_0 = \sqrt[n]{\left(\frac{T_a}{T_n} \right)^3} \cdot \frac{I_{sc}}{-1 + e^{\left[q \frac{V_{pv} + R_s \cdot I_{pv}}{K \cdot T_a} \right]}} \cdot e^{\left[\frac{q \cdot V_g}{n \cdot \left(\frac{1}{T_a} - \frac{1}{T_n} \right)} \right]}, \quad (5)$$

Where n denotes the diode ideality factor. Moreover, the photo-generated current I_{ph} is defined by:

$$I_{ph} = \frac{G_a}{G_n} [I_{sc} + K_I (T_a - T_n)], \quad (6)$$

where T_a is the absolute temperature, T_n is the nominal temperature given at Standard Test Conditions (STC), i.e., $T_n = 25^\circ\text{C}$, K_I is the constant weighting the temperature

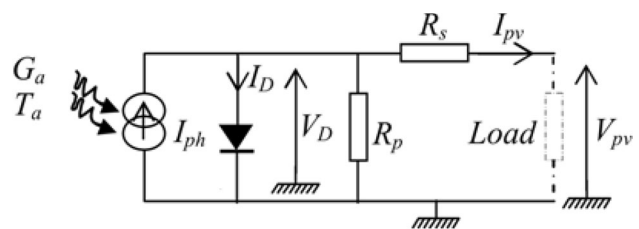


Fig. 1 Equivalent electrical circuit of PV/PVT cells



discrepancy $\Delta T = T_a - T_n$, G_a is the total solar irradiance and G_n is the nominal total solar irradiance given at STC, i.e., $G_n = 1000 \text{ W/m}^2$. According to Eq. (6), the maximum photocurrent I_{phmax} is determined when T_a and G_a reach its nominal values, i.e., $T_a = T_n$, and $G_a = G_n$. It yields in fact $I_{\text{phmax}} = I_{\text{sc}}$. Moreover, the short resistor current I_{sc} is given when the series resistance is low enough and the shunt resistance is high enough. Therefore, I_{ph} should be limited by the upper bound I_{sc} . Table 1 summarizes the meaning and the corresponding value of diverse electrical components.

Formulation of the optimization problem

The desired single diode PV/PVT models have four unknown variables which are regrouped in the following design vector:

$$X = (I_{\text{ph}}, n, R_s, R_p)^T. \quad (7)$$

The optimal vector X^* is determined from minimizing the mean square error (MSE) criterion, in which the fitness function for a sampled point k is given by:

$$J_k(X) = I_{\text{pvm}}(k) - I_{\text{pve}}(k), \quad (8)$$

where $I_{\text{pvm}}(k)$ is the predicted load current determined from Eqs. (3)–(5), $I_{\text{pve}}(k)$ is the sampled load current given through actual PV and PVT systems at sampling time k .

Table 1 Values used in equivalent electrical circuit

Parameter	Quantity identification (unity)	Value
I_{sc}	Short resistor current (A)	2.99
q	Elementary charge (C)	1.60×10^{-19}
K	Boltzmann's constant (J/K)	1.38×10^{-23}
V_{oc}	Open-circuit voltage (V)	20.80
V_g	Energy gap (eV)	1.20

Furthermore, the fitness function of one set of PV/PVT parameters for N sampled points is given by:

$$\min_X J(X) = \min_{X_{\min} < X < X_{\max}} \left\{ \frac{1}{N} \sum_{k=1}^N [I_{\text{pvm}}(k) - I_{\text{pve}}(k)]^2 \right\}. \quad (9)$$

Experimental tests and study cases

The comparative study has been presented here for two solar systems based upon ISOFOTON I-50 PV modules. The first one is the conventional PV cell operating without cooling. However, the second one is the proposed PVT cell that previously reinforced against high temperatures by means of the closed water circuit. These solar systems are positioned on the building roof of the applied research unit in renewable energy located in the south of Algeria.

In this study, both PV and PVT panels are inclined by an angle equals to the latitude of the area and each one has two sensors. The first sensor is a K-type thermocouple which measures the absolute temperature using the Campbell CS215 instrument. The second one is installed to measure the total solar irradiance using the Kipp and Zonen CMP21 pyranometer.

All recorded experimental data are carried out by the Agilent 34970 A. The experimental systems are shown in Fig. 2.

The typical electrical characteristics provided by both solar systems are summarized in Table 2:

Note that, in severe weather conditions, absolute temperatures and total solar irradiances change, respectively, within $31.5^\circ\text{C} \leq T_a \leq 44.5^\circ\text{C}$ and $600 \text{ W/m}^2 \leq G_a \leq 1050 \text{ W/m}^2$. The overheating problem of PVT cells is solved using the proposed cooling system which drops the PVT cell temperatures until those neighboring the nominal temperature range, i.e., $22.3^\circ\text{C} \leq T_a \leq 26.9^\circ\text{C}$. Consequently, the electrical properties provided by the PVT system depend only on a given total solar irradiance range. On the other side, the total solar

Fig. 2 Experimental prototype of PV and PVT systems

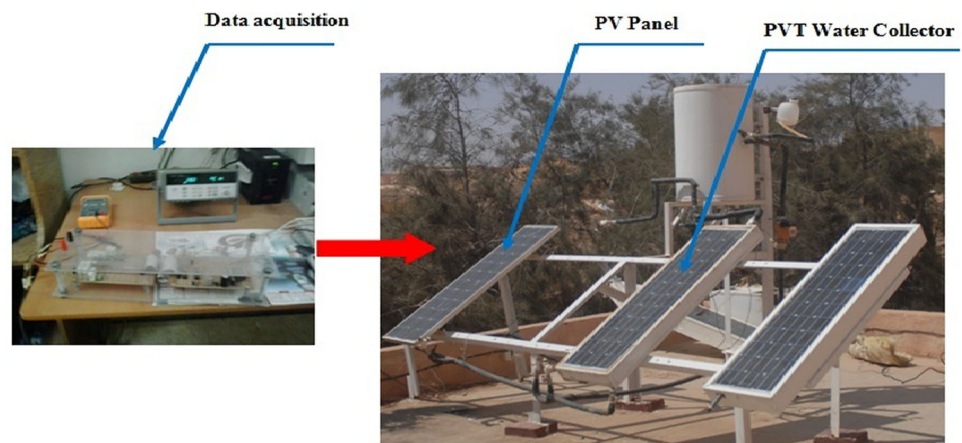


Table 2 Typical electrical characteristics of PV/PVT modules

Characteristic	Value
Maximum power P_{\max}	39.10 W
Maximum voltage V_{\max}	14.90 V
Maximum current I_{\max}	2.620 A
Number of cells	36

irradiance range has been divided on two sub-ranges $650 \text{ W/m}^2 \leq G_a \leq 750 \text{ W/m}^2$ and $800 \text{ W/m}^2 \leq G_a \leq 1050 \text{ W/m}^2$ in which the same obtained electrical properties by the actual PVT system may be conserved. For that reason, two experimental measurements were performed in the modeling phase the actual PVT behavior. These perfect modeling requirements occur in the month of April, especially, from starting times 10h00 and 14h00. For both actual PV and PVT systems, experimental data were recorded every 30 s, in a clear day during the month of April 2015 from 10h00 to 12h30, yielding to 300 sampled measurements. In the same way, a second set of 300 other sampled measurements were recorded from 14h00 to 16h30. Therefore, a total set of $N = 600$ sampled measurements were recorded. During the first $N = 300$ measurements, the mean absolute temperatures and the mean total solar irradiances varied around $T_a = 22.3^\circ\text{C}$ and $G_a = 700.6544 \text{ W/m}^2$, respectively. On the other hand, during the second $N = 300$ measurements the mean absolute temperatures and the mean total solar irradiances varied around $T_a = 26.9^\circ\text{C}$ and $G_a = 900.3362 \text{ W/m}^2$, respectively. The recorded experimental data are then stored in an on-board SD card for an off-line PV and PVT model parameters extraction. Its optimal sets are given by the GA and PSO algorithm using the following lower and upper boundary constraints:

$$\underbrace{\begin{bmatrix} 0 \\ 1 \\ 0 \\ 0 \end{bmatrix}}_{X_{\min}} \leq \begin{bmatrix} I_{ph} \\ n \\ R_s \\ R_p \end{bmatrix} \leq \underbrace{\begin{bmatrix} I_{sc} \\ 2 \\ \inf \\ \inf \end{bmatrix}}_{X_{\max}}. \quad (10)$$

Tables 3 and 4 summarize the tuning parameters of the GA and PSO algorithm, which are given according to some guidelines proposed in [23–25]:

Note that the GA and PSO algorithm are executed 20 times. After that, the best obtained fitness value is considered to design the single diode PV and PVT models.

Design of PV and PVT models

Design of first PV and PVT models

Note that one of most important factors that validate the GA and PSO algorithm is the best value of the fitness function

Table 3 PSO parameters

Parameter	Value
Number of executions of PSO algorithm	20
Swarm size n_p	100
Maximum iteration number I_{\max}	200
Inertia factor c_0	0.90
Cognitive learning rate c_1	0.25
Social learning rate c_2	1.25

Table 4 GA parameters

Parameter	Value
Number of executions of GA	20
Population size	100
Generation number	200
Reproduction	
Elite count	2
Crossover	0.8
Mutation function	Constrain dependent
Crossover function	Scattered
Migration	
Direction	forward
Fraction	0.2

which should be lower as much as possible. Therefore, Fig. 3 shows the obtained fitness plots provided through GA and PSO algorithm during the extraction process of the first PV/PVT model parameters where the best minimization of the cost function is presented by the dashed blue line.

According to Fig. 3, it is easy to observe that the GA converges within 50 generations whereas the PSO algorithm converges within 160 generations yielding also the best MSE minimization. The obtained first PV and PVT model parameters are summarized in Table 5 in which the best parameters are mentioned in bold:

To confirm these results, Fig. 4 compares the actual current–voltage characteristics provided by the proposed PVT system with those determined through its corresponding first PVT models. In addition, Fig. 5 compares the above mentioned characteristics given through the conventional actual PV system and its corresponding first PV models.

According to Figs. 4 and 5, the current–voltage characteristics, provided by actual PV and PVT systems, matched as close as possible with those given by the first PV and PVT models where the best results are ensured by the PSO algorithm. Now, the obtained actual and predicted power–voltage characteristics are compared in Fig. 6:

According to Fig. 6, it is easy to observe that the obtained actual power–voltage characteristics are closely matching those determined through the corresponding models. This



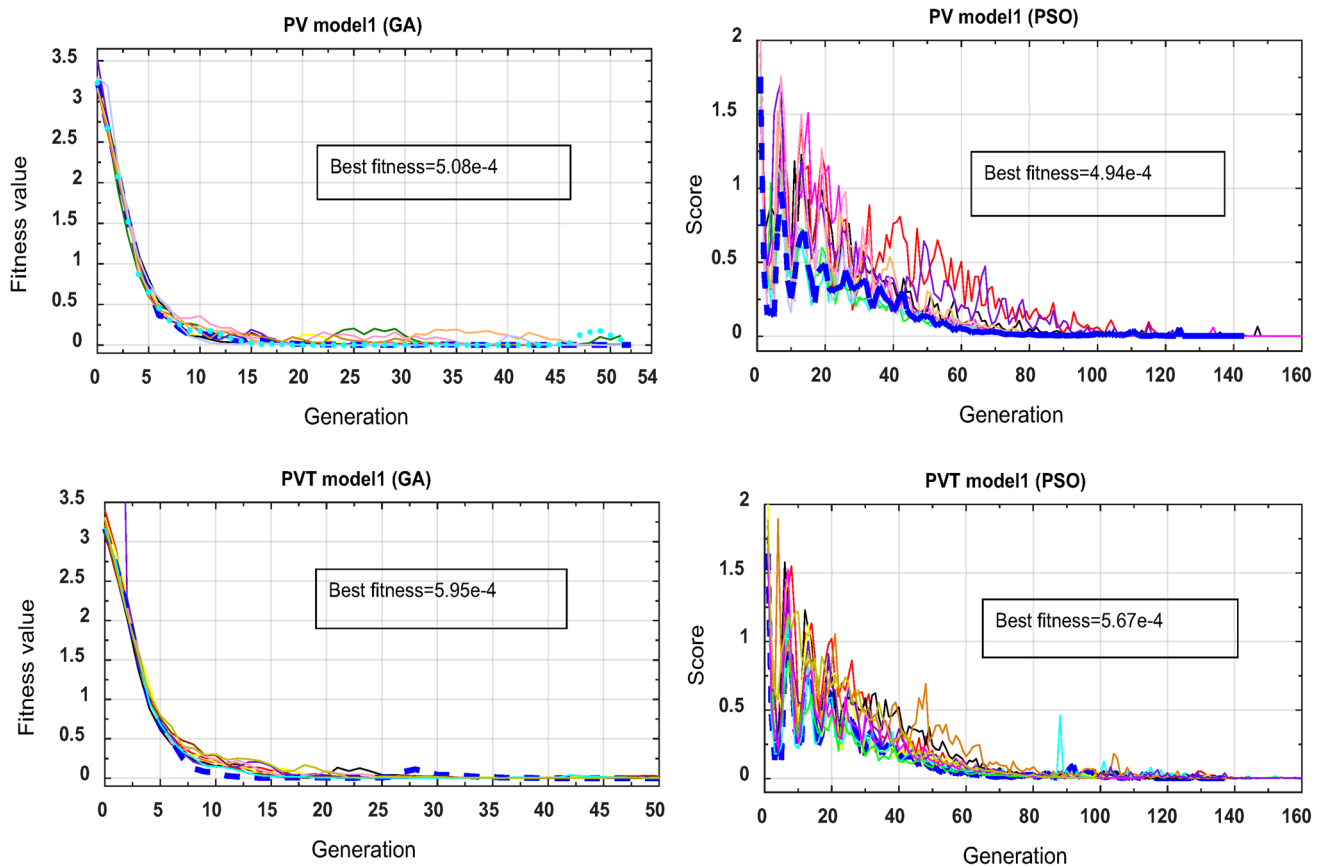


Fig. 3 Obtained fitness curves through GA and PSO algorithm for the first PV/PVT models

Table 5 Identification results of first PV and PVT models

		Model parameters				J_{\min}
		I_{ph}	n	R_s	R_p	
PVT	GA	2.0993	1.0000	0.1817	2.8967	5.95×10^{-4}
	PSO	2.1626	1.0018	0.1936	2.1599	5.67×10^{-4}
PV	GA	1.9728	1.5734	0.0343	4.7437	5.08×10^{-4}
	PSO	2.0180	1.0000	0.1167	3.7548	4.94×10^{-4}

figure confirms also that the obtained power energy is enhanced by the actual PVT system with a maximal value of $P_{PVT} = 26.19$ Watts given at the voltage $V = 14.66$ Volts. This maximal power is better than the one provided by the conventional PV system in which its maximal power reaches $P_{PV} = 25.9$ Watts at the voltage $V = 14.50$ Volts. Note that, this comparison does not reduce the GA efficiency, as it will be shown in the next section.

Design of second PV and PVT models

In this section, the same tuning parameters summarized in Tables 3 and 4 are used. Therefore, Fig. 7 shows the

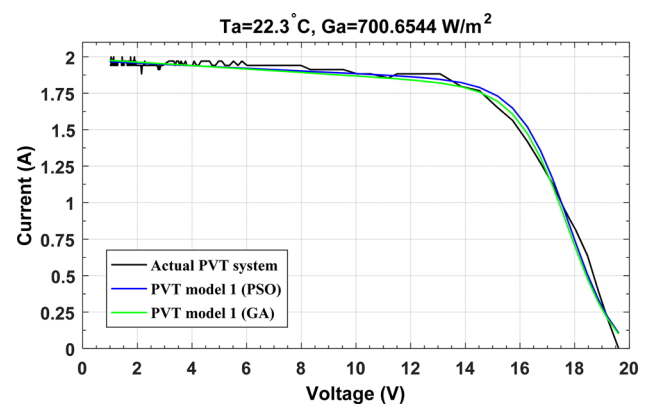


Fig. 4 Obtained current–voltage characteristics by the actual PVT system and its corresponding first PVT model

obtained fitness plots provided through GA and PSO algorithm during the extraction process of the second PV and PVT model parameters where the best minimization of the cost function is presented by the dashed blue line.

According to Fig. 7, it is easy to observe that the best fitness values obtained by GA and PSO algorithm are, respectively, provided within 50 and 175 generations, in which the best results are ensured by the GA. Note, the obtained second PV and PVT model parameters are



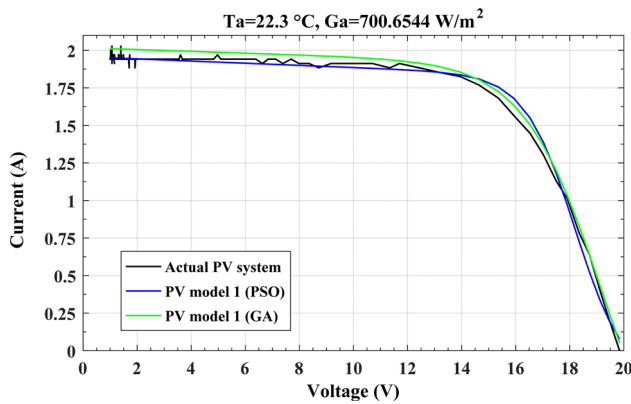


Fig. 5 Obtained current–voltage characteristics by the actual PV system and its corresponding first PV model

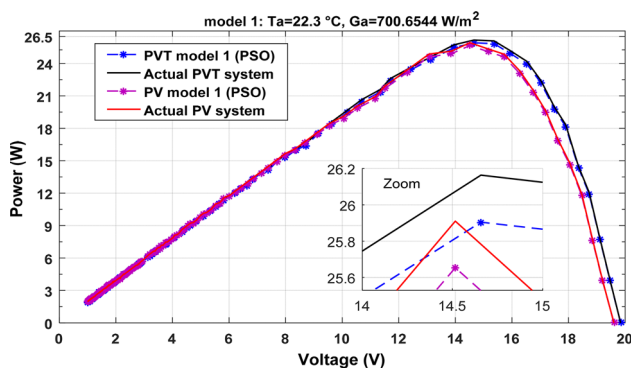


Fig. 6 Obtained power–voltage characteristics by the actual PV and PVT systems and its corresponding first PV and PVT models based upon PSO algorithm

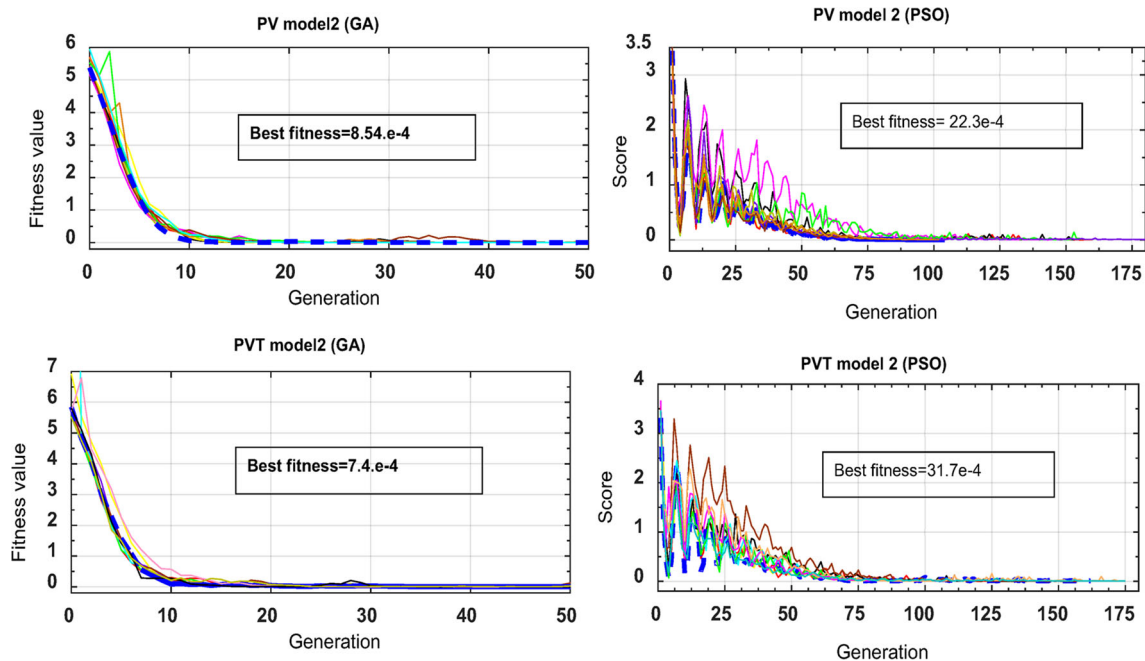


Fig. 7 Obtained fitness curves through GA and PSO algorithm for the second PV/PVT models

summarized in Table 6 in which the best parameters are mentioned in bold.

According to Table 6, it is easy to observe that the best minimization of the MSE criterion is performed by using the GA.

To confirm these results, Fig. 8 compares the actual current–voltage characteristics provided by the proposed PVT system with those determined through its corresponding second PVT models. In addition, Fig. 9 compares the above mentioned characteristics given through the conventional actual PV system and its corresponding second PV models.

According to Figs. 8 and 9, the obtained current–voltage characteristics by the second PV and PVT models are matched as close as possible with those given through the actual PV and PVT systems where the GA gives the best models.

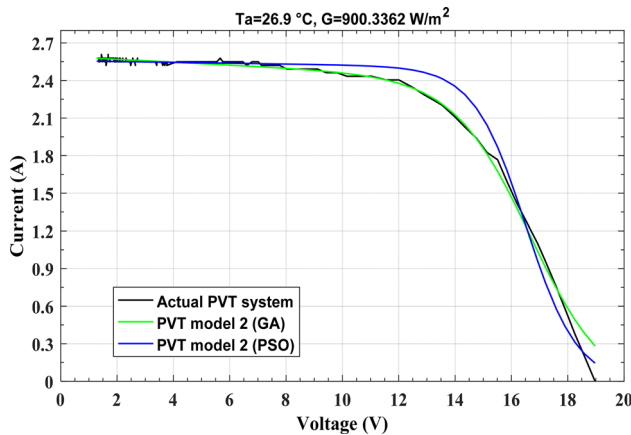
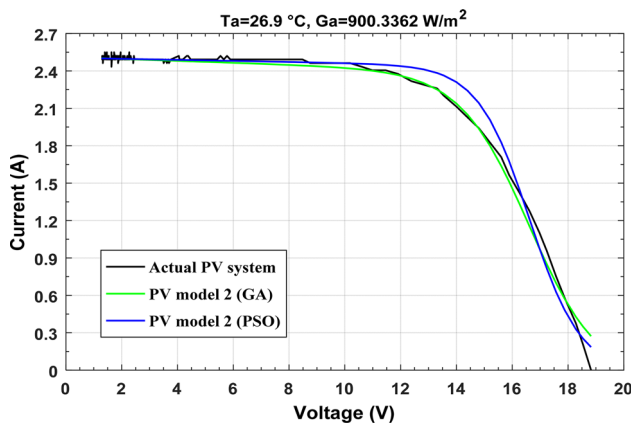
For this reason, only the second PV and PVT models based upon the GA are used to compare its power–voltage characteristics with those determined through the actual PV and PVT systems.

According to Fig. 10, it is clear to observe that the obtained power energy by the actual PVT system has the peak value $P_{PVT} = 30.48$ Watts $V = 13.6$ Volts, which is better than the one provided by the actual PV system in which $P_{PV} = 29.75$ Watts at $V = 13.30$ Volts.



Table 6 Identification results of second PV/PVT models

		Parameters				J_{\min}
		I_{ph}	n	R_s	R_p	
PVT	GA	2.9822	1.4644	0.3237	2.1342	7.40×10^{-4}
	PSO	2.9900	1.0000	1.2007	7.1147	31.70×10^{-4}
PV	GA	2.8508	1.3110	0.4191	3.2142	8.54×10^{-4}
	PSO	2.9900	1.0000	1.0825	5.5967	22.30×10^{-4}

**Fig. 8** Obtained current–voltage characteristics by the actual PVT system and its corresponding second PVT model**Fig. 9** Obtained current–voltage characteristics by the actual PV system and its corresponding second PV model

Validation of the obtained PV and PVT models

In this section, both first PV and PVT models based upon PSO algorithm and both second PV and PVT models based upon GA are validated in severe atmospheric conditions, which are recorded in July 2015.

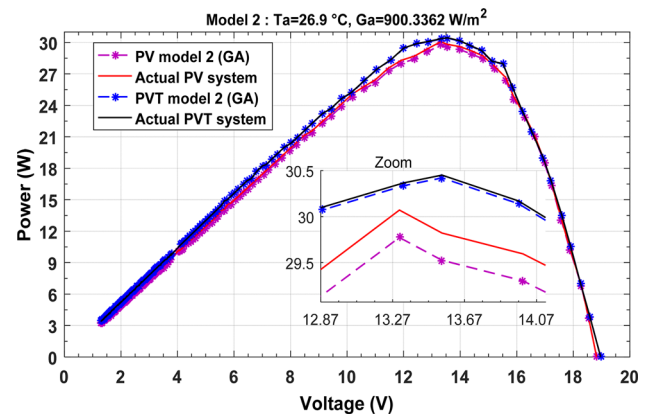
**Fig. 10** Obtained power–voltage characteristics by the actual PV and PVT systems and its corresponding second PV and PVT models based upon GA

Table 7 summarizes the given absolute temperatures and the total solar irradiances at different times.

According to Table 7 the five power–voltage curves obtained by actual PV and PVT systems are compared with those provided by its corresponding models. The proposed comparisons are established according to the given total solar irradiance range. Figures 11 and 12 compare the given power–voltage characteristics provided by actual PV and PVT systems and both first and second PV and PVT models.

According to Figs. 11 and 12 the maximal powers provided by the actual PV and PVT systems can be arranged as the following histogrammes:

Table 8 compares the given maximal powers in different weather conditions.

According to Figs. 13 and 14, it is obvious to confirm the following three main results:

- In high temperatures, the proposed PVT models ensure better robustness properties than those provided by the conventional PV models.
- The proposed PVT models have the ability to well model the actual PVT measurement regardless the severe atmospheric conditions.
- The proposed cooling system ensures the best electrical powers which become stationary in two different irradiation ranges and independently of temperature variations.

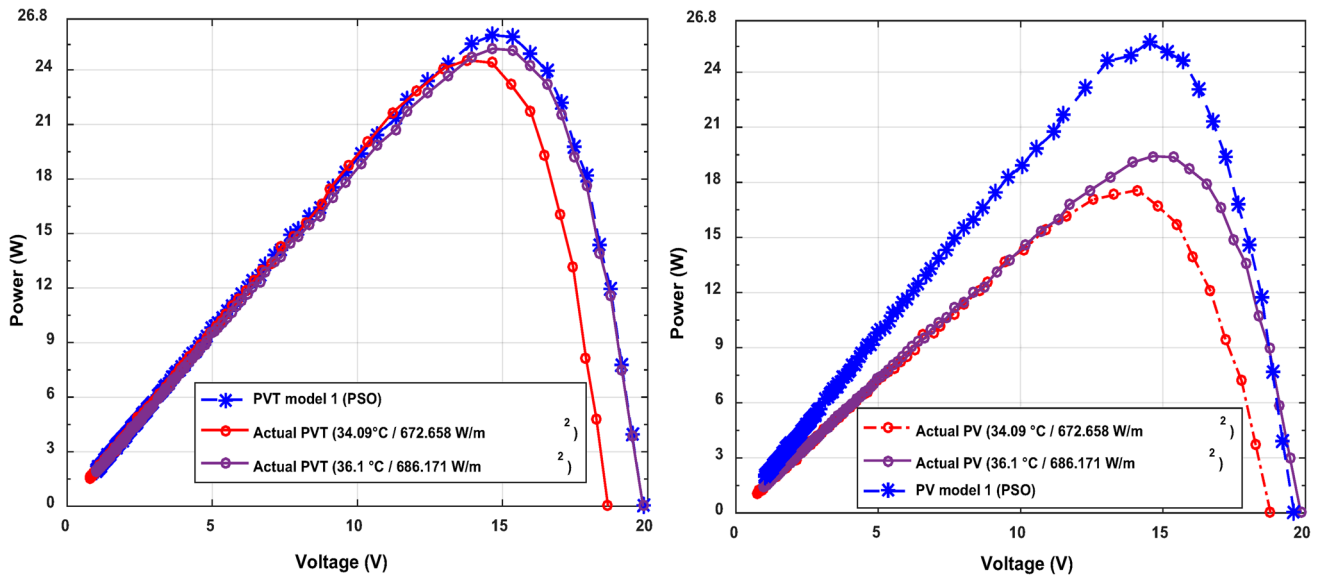
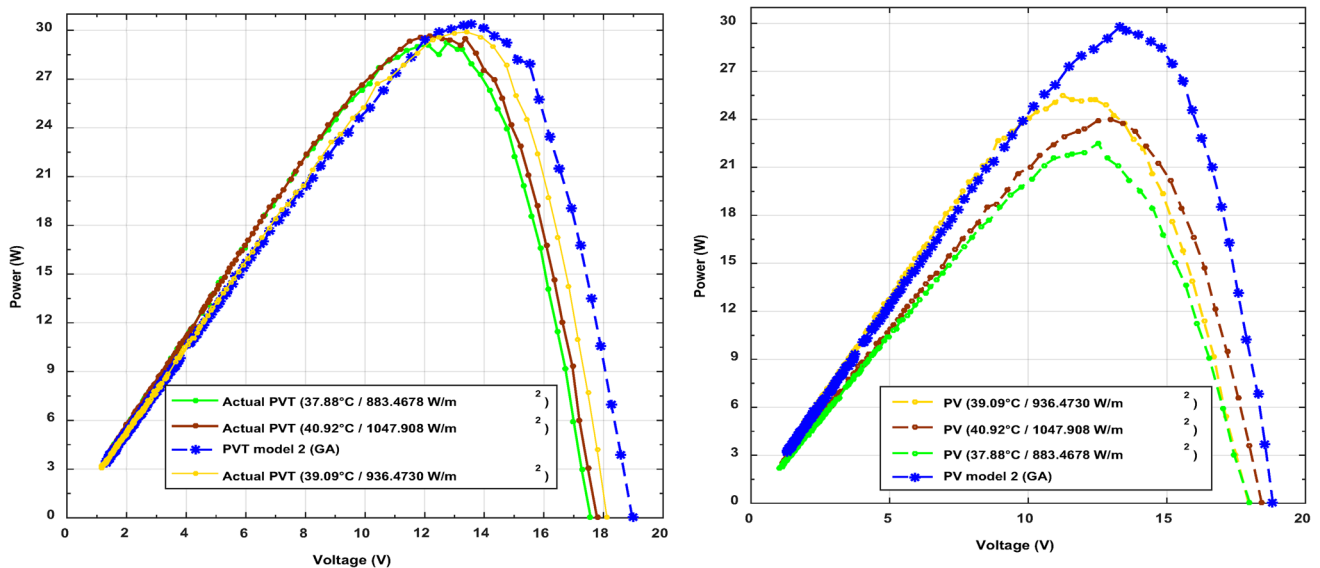
Conclusion

In this paper, the water-cooled PVT system is well modeled by two single diode PVT models according to the two total solar irradiance ranges and the absorbed temperature



Table 7 Absolute temperatures and total solar irradiances used for PV and PVT models validation

Time	08H30	09H00	11H00	13H30	15H30
G_a (W/m ²)	672.6580	686.1710	883.4676	1047.9080	936.4730
T_a (°C)	34.09	36.01	37.88	40.92	39.09

**Fig. 11** Comparison between the actual power–voltage characteristics and those given by the first PV and PVT models using the PSO algorithm**Fig. 12** Comparison between the actual power–voltage characteristics and those given by the second PV and PVT models using the GA

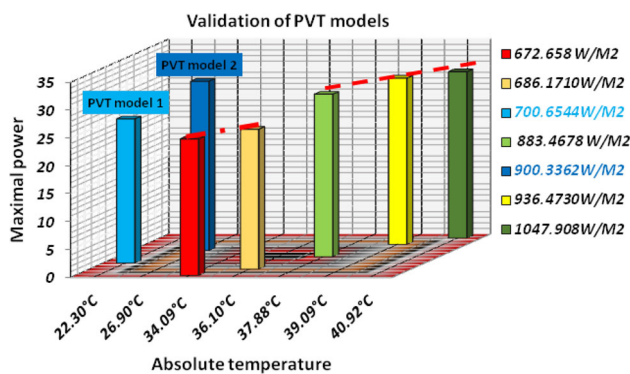
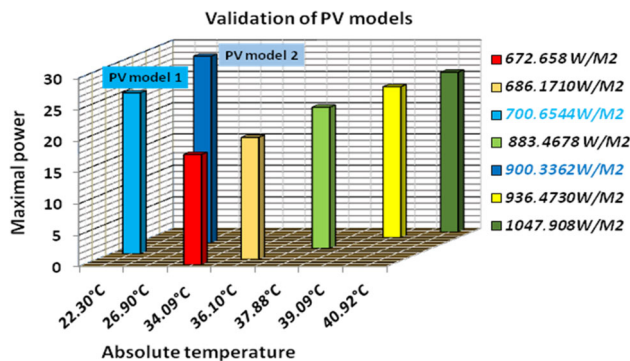
system. The optimal set of the PVT model parameters are identified through experimental data using both evolutionary optimization algorithms such as GA and PSO. The given current–voltage and power–voltage curves by the actual PV and PVT systems are compared to those given by

the proposed PV and PVT models in nominal atmospheric conditions. The robustness of the best PV and PVT models are verified in severe atmospheric conditions in which the PVT model becomes more advantageous than the conventional PV one from an energetic point of view. So, the



Table 8 The obtained maximal powers in different weather conditions compared with those given by the proposed models where the best results are mentioned in bold

G_a (W/m^2)	T_a ($^{\circ}C$)	P_{max} (PVT model1) = 26.19 Watt			P_{max} (PV model1) = 25.90 Watt		
		Actual P_{maxPVT}	Match ratio $P_{maxPVT\%}$	Match ratio error $\xi_{PVT\%}$	Actual P_{maxPV}	Match ratio $P_{maxPV\%}$	Match ratio error $\xi_{PV\%}$
672.658	34.09	24.54	93.700	6.3	17.58	67.87	32.124
686.171	36.10	25.16	96.067	3.93	19.43	75.019	24.981
		P_{max} (PVT model2) = 30.48 Watt			P_{max} (PV model2) = 29.75 Watt		
883.4678	37.88	29.21	95.830	4.166	22.50	75.63	21.008
936.473	39.09	29.90	98.097	1.706	25.47	85.613	14.387
1047.908	40.92	29.68	97.375	2.6247	24.02	80.739	19.261

**Fig. 13** Validation of the PVT models within the severe atmospheric conditions**Fig. 14** Validation of the PV models within the severe atmospheric conditions

proposed PVT model becomes interesting for practical uses.

Acknowledgements The authors would like to thank the anonymous reviewers for their valuable suggestions that enhance the technical and scientific quality of this paper.

Open Access This article is distributed under the terms of the Creative Commons Attribution 4.0 International License (<http://creativecommons.org/licenses/by/4.0/>), which permits unrestricted use, distribution, and reproduction in any medium, provided you give appropriate credit to the original author(s) and the source, provide a link to the Creative Commons license, and indicate if changes were made.

References

- Skoplaki, E., Palyvos, J.: On the temperature dependence of photovoltaic module electrical performance: a review of efficiency/power correlations. *Sol. Energy* **83**(5), 614–624 (2009)
- Alfegi, E.M.A., Sopian, K., Othman, M.Y.H.: Yatim BB (2006) Transient mathematical model of both side single pass photovoltaic thermal air collector. *mh* **0054**, 1 (1000)
- Mazón-Hernández, R., García-Cascales, J.R., Vera-García, F., Káiser, A.S., Zamora, B.: Improving the electrical parameters of a photovoltaic panel by means of an induced or forced air stream. *Int. J. Photoenergy* **2013**, 10 (2013). doi:10.1155/2013/830968
- De Soto, W., Klein, S., Beckman, W.: Improvement and validation of a model for photovoltaic array performance. *Sol. Energy* **80**(1), 78–88 (2006)
- Dolara, A., Leva, S., Manzolini, G.: Comparison of different physical models for PV power output prediction. *Sol. Energy* **119**, 83–99 (2015)
- Kim, K., Shan, Y., Nguyen, X.H., McKay, R.I.: Probabilistic model building in genetic programming: a critical review. *Genet. Program. Evol. Mach.* **15**(2), 115–167 (2014)
- Tabet, I., Touafek, K., Bellel, N., Bouarroudj, N., Khelifa, A., Adouane, M.: Optimization of angle of inclination of the hybrid photovoltaic-thermal solar collector using particle swarm optimization algorithm. *J. Renew. Sustain. Energy* **6**(5), 053116 (2014)
- Askarzadeh, A., dos Santos Coelho, L.: Determination of photovoltaic modules parameters at different operating conditions using a novel bird mating optimizer approach. *Energy Convers. Manag.* **89**, 608–614 (2015)
- Fialho, L., Melício, R., Mendes, V.M.F., Estanqueiro, A., Colares-Pereira, M.: PV systems linked to the grid: parameter identification with a heuristic procedure. *Sustain. Energy Technol. Assess.* **10**, 29–39 (2015)
- Ogliari, E., Bolzoni, A., Leva, S., Mussetta, M.: Day-ahead PV Power Forecast by Hybrid ANN Compared to the Five



- Parameters Model Estimated by Particle Filter Algorithm. In: International Conference on Artificial Neural Networks, pp. 291–298. Springer (2016)
11. Soon, J.J., Low, K.-S.: Optimizing photovoltaic model parameters for simulation. In: Industrial Electronics (ISIE), 2012 IEEE International Symposium on 2012, pp. 1813–1818. IEEE (2012)
 12. Qin, H., Kimball, J.W.: Parameter determination of photovoltaic cells from field testing data using particle swarm optimization. In: Power and Energy Conference at Illinois (PECI), 2011 IEEE 2011, pp. 1–4. IEEE (2011)
 13. Dizqah, A.M., Maheri, A., Busawon, K.: An accurate method for the PV model identification based on a genetic algorithm and the interior-point method. *Renew. Energy* **72**, 212–222 (2014)
 14. Kennedy, J.: Particle swarm optimization. In: Encyclopedia of machine learning. pp. 760–766. Springer, (2011)
 15. Chen, J.-H., Yau, H.-T., Hung, T.-H.: Design and implementation of FPGA-based Taguchi-chaos-PSO sun tracking systems. *Mechatronics* **25**, 55–64 (2015)
 16. Zhang, C., Wu, M., Luan, L.: An optimal PSO distributed pre-coding algorithm in QRD-based multi-relay system. *Future Gener. Comput. Syst.* **29**(1), 107–113 (2013)
 17. Qi, J., Zhang, Y., Chen, Y.: Modeling and maximum power point tracking (MPPT) method for PV array under partial shade conditions. *Renew. Energy* **66**, 337–345 (2014)
 18. Chang, K.K.: Modeling of PV performance without using equivalent circuits. *Sol. Energy* **115**, 419–429 (2015)
 19. Chouder, A., Silvestre, S., Taghezouit, B., Karatepe, E.: Monitoring, modelling and simulation of PV systems using LabVIEW. *Sol. Energy* **91**, 337–349 (2013)
 20. Yatimi, H., Aroudam, E.H.: A Detailed Study and Modeling of Photovoltaic Module under Real Climatic Conditions. (2015)
 21. Eltamaly, A.M., Mohamed, M.A.: A novel software for design and optimization of hybrid power systems. *J. Brazil. Soc. Mech. Sci. Eng.* **38**(4), 1299–1315 (2016)
 22. Hatti, M.: Operation and Maintenance Methods in Solar Power Plants. In: Use, Operation and Maintenance of Renewable Energy Systems. pp. 61–93. Springer, (2014)
 23. Ratnaweera, A., Halgamuge, S.K., Watson, H.C.: Self-organizing hierarchical particle swarm optimizer with time-varying acceleration coefficients. *IEEE Trans. Evol. Comput.* **8**(3), 240–255 (2004)
 24. Perez, R., Behdinan, K.: Particle swarm approach for structural design optimization. *Comput. Struct.* **85**(19), 1579–1588 (2007)
 25. Angelova, M., Pencheva, T.: Tuning genetic algorithm parameters to improve convergence time. *Int. J. Chem. Eng.* **2011**, 7 (2011). doi:[10.1155/2011/646917](https://doi.org/10.1155/2011/646917)

Publisher's Note

Springer Nature remains neutral with regard to jurisdictional claims in published maps and institutional affiliations.

